J Mater Sci (2008) 43:7219–7224
DOI 10.1007/s10853-008-2947-9

Self-organized TiO_2 nanotubes with controlled dimensions by anodic oxidation

Ammar Elsanousi · Jun Zhang · H. M. H. Fadlalla · Feng Zhang · Hui Wang · Xiaoxia Ding · Zhixin Huang · Chengcun Tang

Received: 10 June 2008 / Accepted: 12 August 2008 / Published online: 17 September 2008

Abstract The effect of ammonium fluoride (NH_4F) concentration on the dimensions (length, diameter, and wall thickness) of the self-organized nanotube arrays has been investigated. Results show that varying the concentration of NH_4F exerts a strong effect on changing the dimensions of the as-grown nanotube arrays. The length of the nanotube arrays increases gradually by increasing the concentration up to a maximum length at a concentration of 1.00 wt%, after which the length decreases slightly with the increase in NH_4F concentration. It was also observed that the diameter and wall thickness of the nanotube arrays vary with the change in concentration of NH_4F, where the diameter was found to alter between 80 and 140 nm, and the wall thickness decreases by increasing the NH_4F concentration. These results indicate that it is possible to entirely control the dimensions of the nanotube arrays, by tailoring the concentration of NH_4F besides the anodization time and voltage.

Introduction

Self-organized nanoporous materials with high aspect ratios are of great scientific interest due to their unique properties that allow them to be applied in a variety of functional applications, such as electronic, magnetic, and optical applications [1–5]. In this context, porous TiO_2 nanotube arrays fabricated by anodic oxidation have received considerable attention for their superior semiconducting and photoelectrochemical properties, in addition to their high surface-to-volume ratios provided by the additional area enclosed inside the hollow structure. This makes them practical for many applications such as photocatalysis, photoelectrolysis, photovoltanics, and sensors [6–15].

Since the first report on the formation of nanoporous anodic oxide film of titanium and its alloys by Zwilling et al. [16], the anodic formation of uniform nanotube arrays of TiO_2 in various electrolytes and with different conditions has undergone extensive investigation to further improve the structure and control the dimensions of these highly ordered structures [17–20]. However, controlling the dimensions of these anodic nanotubular arrays and their formation mechanism are still under investigation.

It has been reported that uniform TiO_2 nanotubes arrays with various lengths can be fabricated in hydrofluoric acid (HF), by tailoring the electrochemical conditions (anodization voltage, fluoride concentration, anodization time, and temperature) [19–23]. It is also well known that both, the applied potential and anodization time represent a key factor for controlling the tube diameter and length [24, 25]. However, tailoring just these factors is not enough to fully control the dimensions of the resulting nanotubular arrays. Recently, it was reported that it is possible to slower the chemical etching of titania, which is produced by the hydrolysis reaction at the pore tip due to the acidity of the fluoric solution, by using neutral electrolytes containing NH_4F instead of HF, thus obtaining high aspect-ratio self-organized TiO_2 nanotubes with lengths up to some micrometers [26–28].

Yoriya et al. [21], studied the effect of the HF concentration in a dimethyl sulfoxide (DMSO) electrolyte on the

---

A. Elsanousi (✉) · J. Zhang · H. M. H. Fadlalla · F. Zhang · H. Wang · X. Ding · Z. Huang · C. Tang (✉)
College of Physical Science and Technology, Central China Normal University, Wuhan 430079, People's Republic of China
e-mail: a.elsanousi@phy.ccnu.edu.cn

C. Tang
e-mail: cctang@phy.ccnu.edu.cn

nanotube dimensions and proved that the concentration of HF has a strong effect on the nanotube length. On the other hand, Xiao et al. [22] reported the formation of nanotube arrays in different electrolytes and demonstrated that organic electrolytes have a tendency to grow longer tubes due to the reduction of water content, which reduces the solubility of TiO_2 and thus promotes the growth of longer tubes.

The aim of this work is to control the dimensions of the self-organized nanotube arrays produced by anodization; therefore, we investigated the influence of NH_4F concentration in ethylene glycol and aqueous electrolytes by tailoring the concentration in a wide range (0.25–1.5 wt%). Experimental results show that varying the concentration of NH_4F exerts a strong effect on changing the dimensions of the as-grown nanotube arrays.

Experimental

Titanium foils (99.6% purity, Tite Inc., Shanghai), with a thickness of 0.25 mm, were chemically etched in 30% HCl solution for 30 min at 80 °C, then rinsed with deionized water, and dried in air. The anodization was carried out in a two-electrode electrochemical cell, with a graphite counter electrode. The foils were anodized at constant voltage of 60 V for 60 min in an electrolyte of ethylene glycol containing ammonium fluoride (NH_4F) with different concentrations. The concentration of NH_4F in the electrolyte was varied from 0.25 to 1.50 wt% with an increment step of 0.25 wt% each time. The anodized samples were then rinsed in deionized water, and degreased by sonicating in 1:1 solution of ethanol and acetone for 3 min, followed by washing again with deionized water and drying in air.

For comparison reason, and to investigate the effect of NH_4F concentration in aqueous electrolytes, the same procedure was performed with an aqueous electrolyte containing ethylene glycol and water in a ratio of 3:2, respectively, at a constant voltage of 20 V and anodization time of 60 min.

The surface morphology and dimension characterization (top-view and cross-section view) of the anodized samples were observed by scanning electron microscopy (SEM, JEOL JSM-6700F). The cross-section images were taken from mechanically cut samples. The crystallographic structure of the produced nanotube arrays, before and after annealing, was determined by X-ray diffraction (XRD) with Cu kα radiation ($\lambda = 1.54178$ Å).

Results and discussion

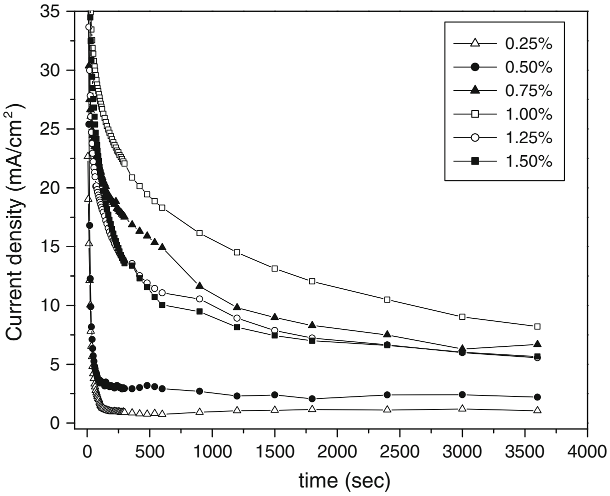

Fig. 1 Current density–time curves for ethylene glycol electrolyte containing NH_4F with different concentrations (0.25–1.50 wt%)

Figure 1 shows the current density versus time behavior during anodization, for the ethylene glycol electrolyte with different NH_4F concentrations. From this figure, it is apparent that all curves exhibit a similar behavior with the time.

In the early stages of the anodization process, a thin oxide layer is formed on the surface of the titanium sheet according the following chemical reaction:

$$Ti + 2H_2O \rightarrow TiO_2 + 4H^+ + 4e^- \quad (1)$$

This compact oxide layer on the titanium surface leads to a rapid reduction in the current density due to its poor electrical conductivity. The current density then reaches a quasi-steady state due to the chemical dissolution of the

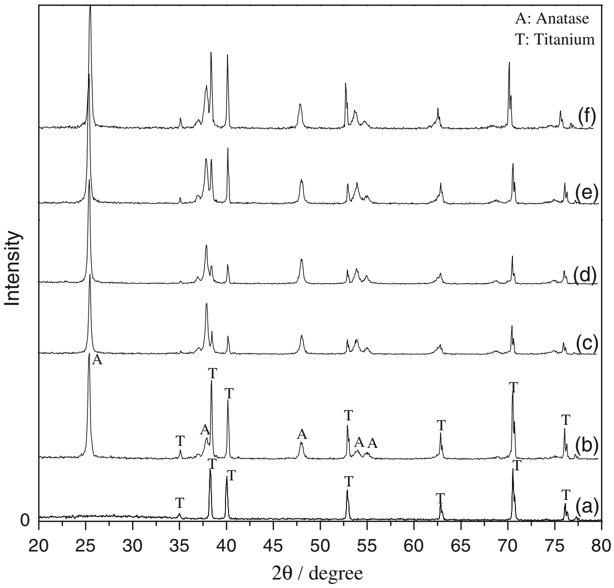

Fig. 2 XRD pattern of TiO_2: (a) before annealing and (b–f) after annealing at 450 °C for 2 h with different NH_4F concentrations (b) 0.50; (c) 0.75; (d) 1.00; (e) 1.25; and (f) 1.50 wt%

oxide layer forming soluble fluoride complexes according to the following reaction:

$$\mathrm{TiO_2} + 6\mathrm{F}^- \rightarrow \mathrm{TiF}_6^{2-} \qquad (2)$$

As a result fine pits or pores are formed at the surface. Under sufficient applied voltage magnitude, field-assisted oxidation occurs at the TiO_2/Ti interface, where the oxygen ions (O^{2-}) are transported from the solution to the oxide layer. At the same time, titanium ions (Ti^{4+}) are transported from the titanium to the oxide/solution interface and dissolve into the solution, leading to a continuous increase in the depth of the porous structure and thus the formation of ordered nanotubes oriented vertically to the substrate [29, 30].

It was also observed from Fig. 1, that the current density behavior with the increasing concentration of NH_4F is divided into two stages: in the first stage, at concentrations between 0.25 and 1.00 wt%, high current densities are obtained, which increase by increasing the concentration. This can be ascribed to the high diffusivity and ion concentration in the electrolyte due to the continuous increase of NH_4F concentration in the electrolyte, leading to an enhancement in the conductivity of the solution. In the second stage and for higher concentrations

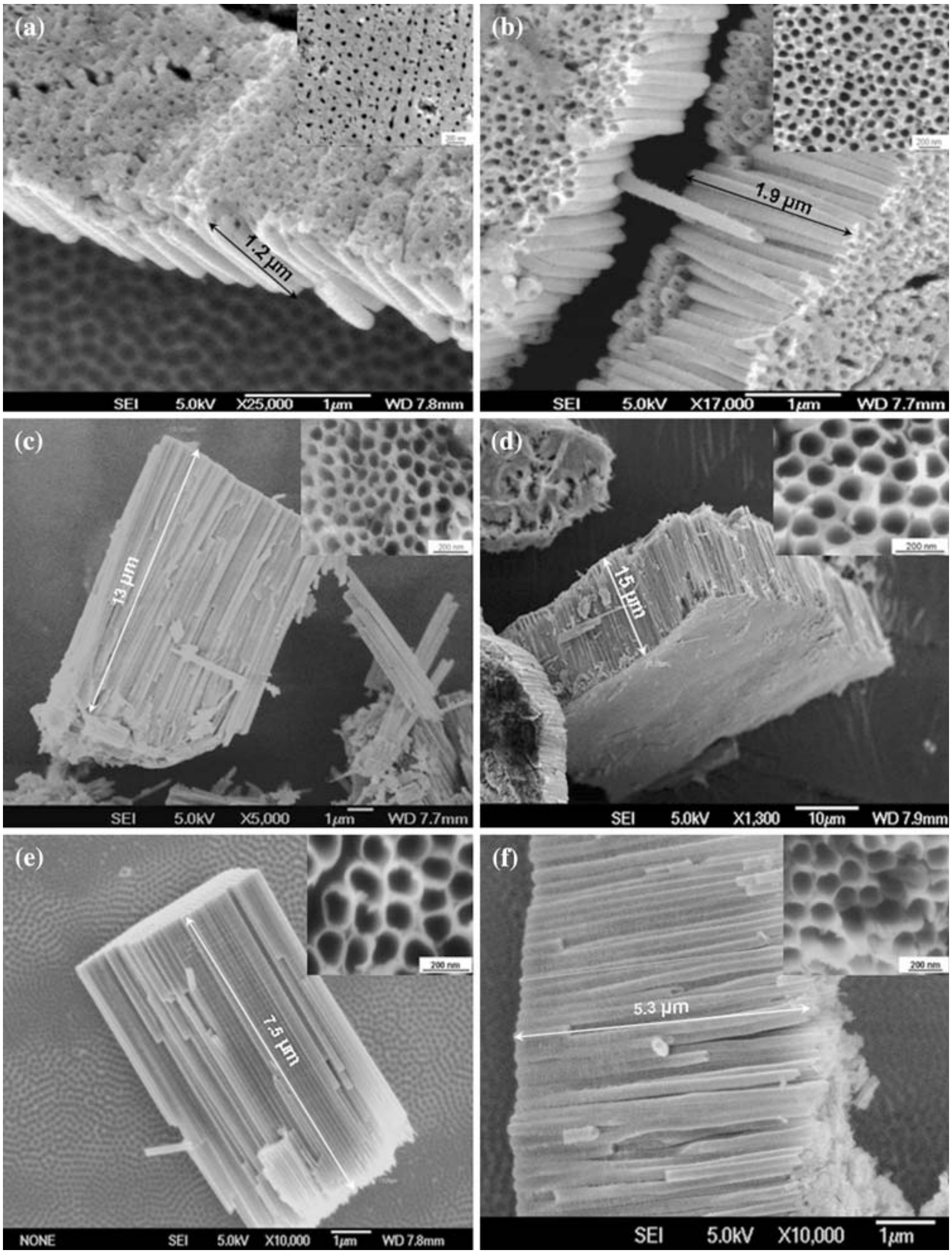

Fig. 3 SEM cross-section images of the samples anodized in ethylene glycol electrolyte at 60 V for 60 min with different NH_4F concentrations: (**a**) 0.25; (**b**) 0.50; (**c**) 0.75; (**d**) 1.00; (**e**) 1.25; and (**f**) 1.50 wt%, Insets are top view of the samples

(1.25–1.50 wt%), the current density drastically falls to values much lower than those at a concentration of 1.00 wt%, which can be attributed to the fast chemical etching of the grown nanotubes, resulting in the formation of shorter nanotubes with reduced ionic conduction.

Figure 2 shows the XRD patterns of the TiO_2 nanotube arrays produced in ethylene glycol electrolyte with different NH_4F concentrations (before and after annealing). Before annealing, the XRD patterns showed that the structure of the as-grown nanotube arrays exposes an amorphous structure, where only Bragg reflections from the titanium substrate can be seen. After annealing at 450 °C, the structure of the nanotube arrays is converted into a crystalline structure, where sharp peaks of anatase phase are observed in all the annealed samples.

Figure 3 shows the SEM images of the samples anodized in ethylene glycol electrolyte with different NH_4F concentrations. SEM observations showed that the as-grown nanotube arrays have very smooth walls and vary in length depending on the concentration of NH_4F in the electrolyte. At a concentration of 0.25 wt%, nanotube arrays with average length of 1.2 μm are obtained (Fig. 3a). Increasing the concentration to 0.50 wt% resulted in a slight increase in the nanotube array length, where nanotubes with an average length of 1.9 μm are obtained as shown in Fig. 3b. At a concentration of 0.75 wt%, a leap in

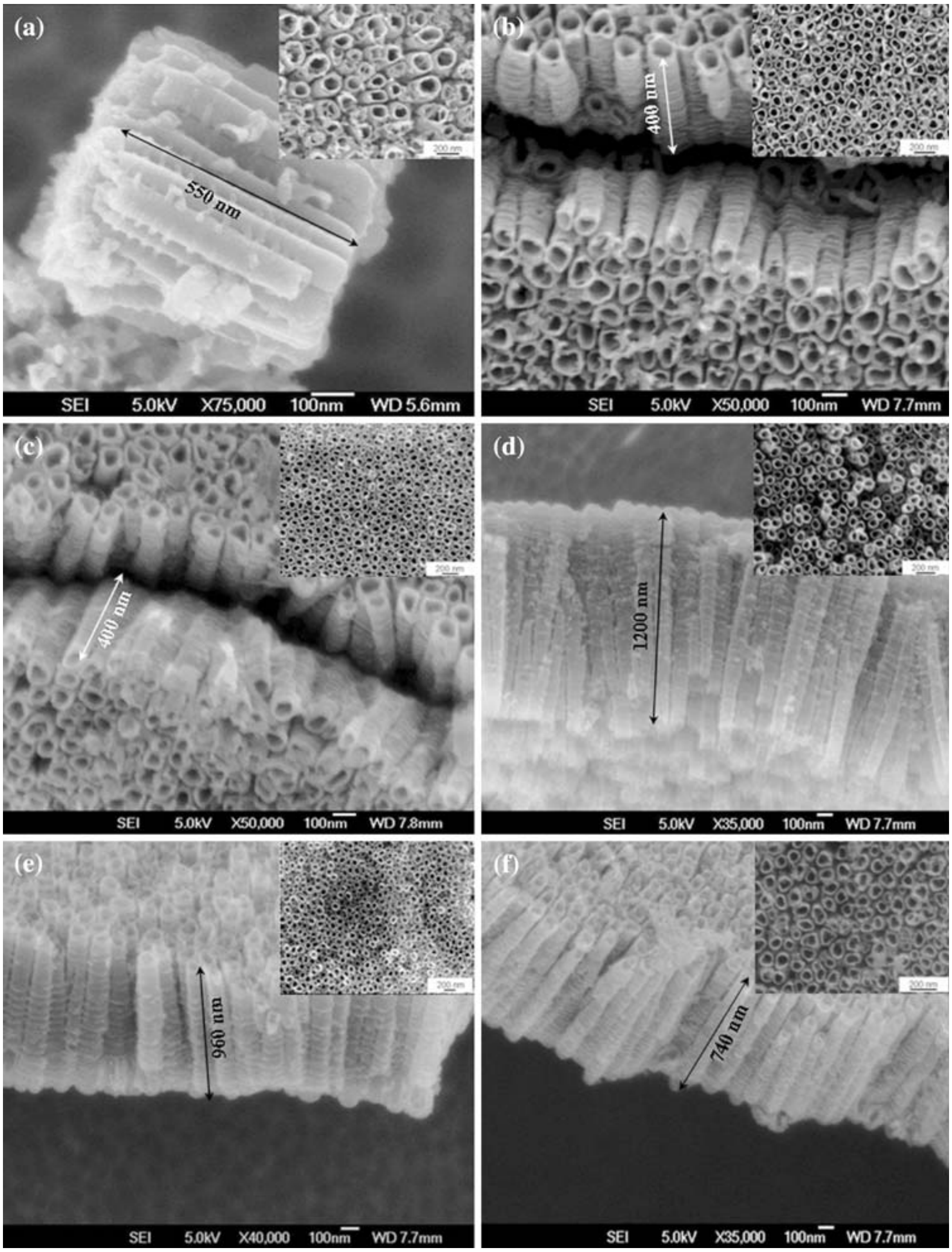

Fig. 4 SEM cross-section images of the samples anodized in aqueous electrolyte at 20 V for 60 min with different NH_4F concentrations: (**a**) 0.25; (**b**) 0.50; (**c**) 0.75; (**d**) 1.00; (**e**) 1.25; and (**f**) 1.50 wt%, Insets are top view of the samples

the length of the nanotube arrays was observed and nanotubes with lengths up to 13 µm are obtained (Fig. 3c). At a concentration of 1.00 wt%, the nanotube arrays reach a maximum length of about 15 µm as can be seen from Fig. 3d. Further increase in the concentration, leads to slight decrease in the length of the nanotube arrays, where the samples with NH_4F concentrations of 1.25 and 1.50 wt% revealed nanotube arrays with lengths of 7.5 and 5.3 µm, respectively (see Fig. 3e, f). This result agrees with the result obtained by Yoriya et al. [21], when varying the concentration of HF in DMSO electrolyte, in which they ascribed to the relatively fast chemical etching of TiO_2 at high acid concentrations, thus resulting in shorter nanotube arrays.

In comparison to aqueous electrolytes containing ethylene glycol and water in the ratio of 3:2, respectively, the same behavior was observed. However, shorter nanotubes were formed as can be seen from Fig. 4. The length of the as-grown nanotube arrays was found to change with NH_4F concentration in the same manner, where at concentrations between 0.25 and 1.00 wt%, nanotube arrays with lengths ranging from 550 to 1200 nm are observed (Fig. 4a–d), while at higher concentrations of 1.25 and 1.50 wt%, nanotube arrays with length of 960 and 740 nm, respectively, are produced, as shown in Fig. 4e and f.

Figure 5 summarizes the average length of the nanotube arrays as a function of the concentration, for ethylene glycol electrolyte (Fig. 5a) and for aqueous electrolyte (Fig. 5b). Both electrolytes expose a maximum length of the nanotube arrays at a concentration of 1.00 wt%. This leads us to the prediction that the concentration of 1.00 wt% is optimal for achieving longer nanotube arrays. Based on previous reports that extending the anodization time results in increasing the nanotube arrays length [9], we believe that it is possible to obtain much longer nanotube arrays at a concentration of 1.00 wt% by extending the anodization time.

It was also observed for the ethylene glycol electrolyte that both the pore diameter and wall thickness of the nanotubes vary with the concentration of NH_4F. The average pore diameter was found to vary between 80 and 140 nm, possibly due to the fluctuations in the dissolution of the oxide layer. The wall thickness was found to decrease by increasing NH_4F concentration, where it starts with an average value of about 40 nm at a concentration of 0.25 wt% and decreases gradually with the increase of the concentration until it reaches 9 nm at concentration of 1.50 wt%, as can be seen in the inset of Fig. 5a. This phenomenon can be ascribed to the increase in the dissolution rate, which increases by the increase of the F^- ions stimulated by increasing the concentration of NH_4F in the electrolyte, leading to an increase in the inner diameter and thus reducing the wall thickness of the nanotubes.

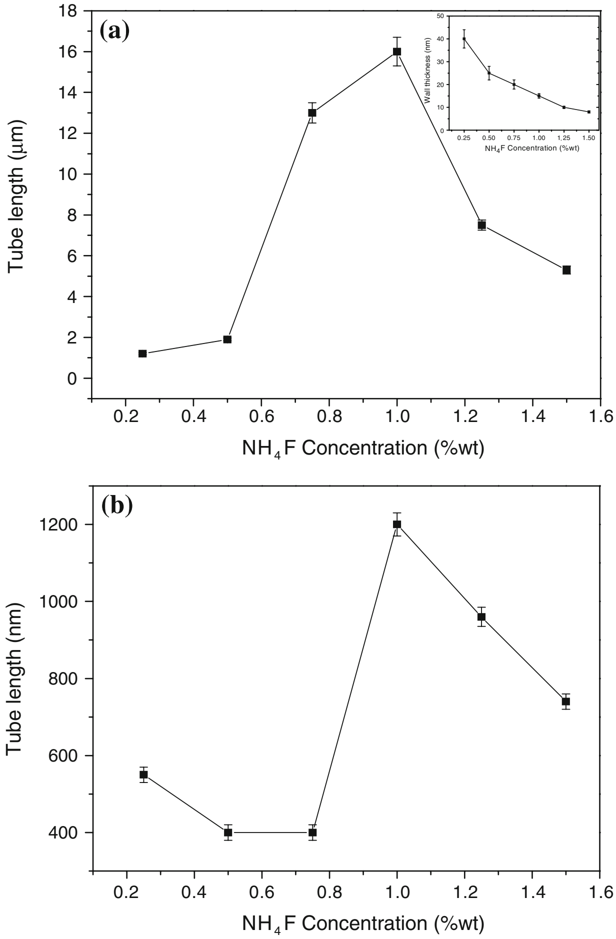

Fig. 5 Variation of the nanotube array length as a function of NH_4F concentration: (**a**) in ethylene glycol electrolyte (inset: variation of the wall thickness as a function of NH_4F concentration) and (**b**) in aqueous electrolyte

Conclusion

In this study, we investigated the influence of NH_4F concentration on the dimensions of the self-organized nanotube arrays produced by anodization in ethylene glycol and aqueous electrolytes. The concentration of NH_4F was varied from 0.25 to 1.50 wt%, while keeping all other electrochemical conditions constant. The results showed that changing the concentration of NH_4F either in ethylene glycol or aqueous electrolytes exerts a strong effect on the overall dimensions of the as-grown nanotube arrays produced by anodization, where varying the concentration of NH_4F does not only affect the length of the nanotube arrays, but also the pore diameter and wall thickness. Increasing the concentration resulted in an increase in the length of the nanotube arrays until it reaches a maximum length at a concentration of 1.00 wt%. Above this concentration, the length of the nanotube arrays decreases slightly with the increase of NH_4F concentration. It was also observed that the diameter and wall thickness of the nanotubes vary with the concentration of NH_4F, where the diameter was found to vary between 80 and 140 nm and the wall thickness decreased with the increase of NH_4F concentration.

These results indicate that it is possible to improve the dimensions of the nanotube arrays by tailoring the concentration of NH_4F besides the anodization time and voltage.

Acknowledgements The authors gratefully acknowledge the financial support for this work from the Fok Fing Tong Education Foundation (Grant No. 91050), and the National Natural Science Foundation of China (Grant No. 50202007).

References

1. Park S, Lim JH, Chung SW, Mirkin CA (2004) Science 303:348. doi:10.1126/science.1093276
2. Sieber I, Hildebrand H, Friedrich A, Schmuki P (2006) J Electroceram 16:35. doi:10.1007/s10832-006-4351-7
3. Lee SB, Mitchell DT, Trofin L, Nevanen TK, Soderlund H, Martin CR (2002) Science 296:2198. doi:10.1126/science.1071396
4. Munoz AG, Chen Q, Schmuki P (2007) J Solid State Electrochem 11:1077. doi:10.1007/s10008-006-0241-9
5. Munoz AG (2007) Electrochim Acta 52:4167. doi:10.1016/j.electacta.2006.11.035
6. Adachi M, Murata Y, Harada M, Yoshikawa Y (2000) Chem Lett 29:942. doi:10.1246/cl.2000.942
7. Chu SZ, Inoue S, Wada K, Li D, Haneda H, Awatsu S (2003) J Phys Chem B 107:6586. doi:10.1021/jp0349684
8. Varghese OK, Gong D, Paulose M, Ong KG, Dickey EC, Grimes CA (2003) Adv Mater 15:624. doi:10.1002/adma.200304586
9. Mor GK, Carvalho MA, Varghese OK, Pishko MV, Grimes CA (2004) J Mater Res 19:628. doi:10.1557/jmr.2004.19.2.628
10. Paulose M, Varghese OK, Mor GK, Grimes CA, Ong KG (2006) Nanotechnology 17:398. doi:10.1088/0957-4484/17/2/009
11. Mor GK, Shankar K, Varghese OK, Grimes CA (2004) J Mater Res 19:2989. doi:10.1557/JMR.2004.0370
12. Uchida S, Chiba R, Tomiha M, Masaki N, Shirai M (2002) Electrochemistry 70:418
13. Adachi M, Murata Y, Okada I, Yoshikawa Y (2003) J Electrochem Soc 150:G488. doi:10.1149/1.1589763
14. Paulose M, Shankar K, Varghese OK, Mor GK, Hardin B, Grimes CA (2006) Nanotechnology 17:1. doi:10.1088/0957-4484/17/1/001
15. Zhang Z, Yuan Y, Fang Y, Liang L, Ding H, Shi G, Jin L (2007) J Electroanal Chem 610:179. doi:10.1016/j.jelechem.2007.07.028
16. Zwilling V, Darque-Ceretti E, Boutry-Forveille A, David D, Perrin MY, Ancouturier M (1999) Surf Interface Anal 27:629. doi:10.1002/(SICI)1096-9918(199907)27:7<629::AID-SIA551>3.0.CO;2-0
17. Mor GK, Verghese OK, Paulose M, Shankar K, Grimes CA (2006) Sol Energy Mater Sol Cells 90:20011. doi:10.1016/j.solmat.2006.04.007
18. Gong D, Grimes CA, Varghese OK, Hu W, Singh RS, Chen Z, Dickey EC (2001) J Mater Res 16:3331. doi:10.1557/JMR.2001.0457
19. Cai Q, Paulose M, Varghese OK, Grimes CA (2005) J Mater Res 20:230. doi:10.1557/JMR.2005.0020
20. Macak JM, Taveira LV, Tsuchiya H, Sirotna K, Macak J, Schmuki P (2006) J Electroceram 16:29. doi:10.1007/s10832-006-3904-0
21. Yoriya S, Paulose M, Varghese OK, Mor GK, Grimes CA (2007) J Phys Chem C 111:13770. doi:10.1021/jp074655z
22. Xiao P, Garcia BB, Guo Q, Liu D, Cao G (2007) Electrochem Commun 9:2441. doi:10.1016/j.elecom.2007.07.020
23. Macak JM, Schmuki P (2006) Electrochim Acta 52:1258. doi:10.1016/j.electacta.2006.07.021
24. Bauer S, Kleber S, Schmuki P (2006) Electrochem Commun 8:1321. doi:10.1016/j.elecom.2006.05.030
25. Prida VM, Manova E, Vega V, Hernandez-Velez M, Aranda P, Pirota KR, Vazquez M, Ruiz-Hitzky E (2007) J Magn Magn Mater 316:110. doi:10.1016/j.jmmm.2007.02.021
26. Macak JM, Tsuchiya H, Schmuki P (2005) Angew Chem Int Ed 44:2100. doi:10.1002/anie.200462459
27. Paulose M, Shankar K, Yoriya S, Prakasam HE, Varghese OK, Mor GK, Latempa TA, Fitzgerald A, Grimes CA (2006) J Phys Chem B 110:16179. doi:10.1021/jp064020k
28. Ghicov A, Tsuchiya H, Macak JM, Schmuki P (2005) Electrochem Commun 7:505. doi:10.1016/j.elecom.2005.03.007
29. Yang DJ, Kim HG, Cho SJ, Choi WY (2008) Mater Lett 62:775. doi:10.1016/j.matlet.2007.06.058
30. Macak JM, Tsuchiya H, Ghicov A, Yasuda K, Hahn R, Bauer S, Schmuki P (2007) Curr Opin Solid State Mater Sci 11:3. doi:10.1016/j.cossms.2007.08.004